Journal of Experimental Botany, Vol. 77, No. 2 pp. 330–344, 2026
https://doi.org/10.1093/jxb/eraf433 Advance Access Publication 30 September 2025

TECHNICAL INNOVATION

A tRNA-gRNA multiplexing system for CRISPR genome editing in *Marchantia polymorpha*

Eftychios Frangedakis*†, Nataliya E. Yelina‡,§, Satish Kumar Eeda¶, Facundo Romani, Alexandros Fragkidis, Jim Haseloff, and Julian M. Hibberd**

Department of Plant Sciences, University of Cambridge, Cambridge CB 3EA, UK

* Correspondence: efragedakis@gmail.com
**Present address: Bristol Medical School, University of Bristol, Dorothy Hodgkin Building, Whitson Street, Bristol, BS1 3NY, UK.
† Present address: School of Life Science, Rikkyo University, Nishi-Ikebukuro, Tokyo, 171-8501, Japan.
‡ Present address: Crop Science Centre, University of Cambridge, 93 Lawrence Weaver Road, Cambridge, CB3 0LE, UK.
§ Present address: Centre for Plant Sciences, University of Leeds, Woodhouse Lane, Leeds, LS2 9JT, UK.
¶ Present address: Crop Transformation, NIAB, Park Farm, Villa Road, Histon, Cambridge, CB24 9NZ, UK.

Received 4 July 2025; Accepted 12 September 2025

Editor: James Murray, Cardiff University, UK

Abstract

The liverwort *Marchantia polymorpha* is a widely used model organism for studying land-plant biology, and it has also proven to be a promising testbed for bioengineering. CRISPR/Cas9 technology has become a transformative tool for precise genome modifications in *M. polymorpha*; however, a robust method for the simultaneous expression of multiple gRNAs, which is crucial for enhancing the versatility of CRISPR/Cas9-based genome editing, has yet to be fully developed. In this study, we introduce an adaptation from the OpenPlant kit CRISPR/Cas9 tools that facilitates expression of multiple gRNAs from a single transcript through incorporation of tRNA sequences. The ability to deliver multiple gRNAs simultaneously significantly improves the capacity and scalability of genome editing in *M. polymorpha*. Additionally, by combining this vector system with a simplified and optimized protocol for thallus transformation, we further streamline the generation of CRISPR/Cas9 mutants in *M. polymorpha*. The resulting gene-editing system offers a multipurpose, time-saving, and straightforward tool for advancing functional genomics in *M. polymorpha*, enabling more comprehensive genetic modifications and genome engineering.

Keywords: CRISPR, genome editing, liverwort, *Marchantia polmorpha*, thallus transformation, tRNA.

Introduction

Marchantia polymorpha represents a powerful model organism for investigating various aspects of plant biology, including genetics, cell biology, development, and evolution (Kohchi *et al.*, 2021; Bowman *et al.*, 2022; Naramoto *et al.*, 2022). It is also an excellent chassis for bioengineering, offering a unique combination of well-established genetic modification tools, a simple body plan, rapid growth, and remarkable regenerative capacity, as well as minimal cultivation requirements (Ishizaki *et al.*, 2016; Boehm *et al.*, 2017; Sauret-Güeto *et al.*, 2020; Frangedakis *et al.*, 2021; Romani *et al.*, 2024; Tse *et al.*, 2024). All these make it an ideal platform for a wide range of synthetic biology applications, such as reprogramming cell

fate, engineering of biosynthetic pathways, development of biosensors, CRISPR-based DNA-recording device systems, and CRISPR-based multiplex gene regulation systems (Gupta and Karkute, 2021; Donà *et al.*, 2023; Kocaoglan *et al.*, 2023; Tansley *et al.*, 2024; Forestier *et al.*, 2025, Preprint).

The compact genome and haploid dominant life cycle of *M. polymorpha* make it particularly well suited for studying genetics (Kohchi *et al.*, 2021). As a result, it is uniquely positioned for exploring fundamental genetic processes, with potential to enhance our understanding of key traits that are conserved across land plants. Genetics has been profoundly transformed by the development of CRISPR technology, which enables precise and targeted genetic modifications by inducing deletions or insertions at specific loci within the nuclear genome (Jinek *et al.*, 2012; Cong *et al.*, 2013; Ran *et al.*, 2013). This gene-editing system utilizes a guide RNA (gRNA) to direct a nuclease protein, such as Cas9, to a specific DNA sequence, where it induces a double-strand break, allowing for accurate genome editing (Ran *et al.*, 2013; Adli, 2018). CRISPR has facilitated significant advances in functional genomics, where the specific manipulation of a sequence allows a better understanding of gene function, and the technology is routinely used in *M. polymorpha* (Sugano *et al.*, 2018, 2014; Sauret-Güeto *et al.*, 2020). One of the challenges in CRISPR-based technologies, including in *M. polymorpha*, is the expression of multiple gRNAs as a single transcript, particularly for applications requiring simultaneous editing of multiple genomic sites. Current CRISPR/Cas9 systems in *M. polymorpha* enable only limited multiplex genome editing or require multiple plasmids with different antibiotic resistance, typically allowing the expression of no more than two gRNAs simultaneously (Sugano *et al.*, 2018, 2014; Sauret-Güeto *et al.*, 2020). Expressing multiple gRNAs using a tRNA-mediated multiplex gRNA expression construct (tRNA-gRNA) is an approach that has been successfully applied in several plant species (Xie, Minkenberg, and Yang, 2015; Hui *et al.*, 2019; Wang *et al.*, 2021). In this system (Fig. 1A), tRNA-gRNA synthetic transcripts mimic native tRNAsnoRNA43 transcripts in plants, allowing endogenous cellular machinery (i.e. RNase P and Z) to cleave the tRNA structure and release mature functional single gRNAs (Fig. 1B) (Xie *et al.*, 2015; Čermák *et al.*, 2017; Ma *et al.*, 2019). Additionally, the tertiary triple-helix structure of the tRNAs is known to contribute to transcript stability (Wilusz *et al.*, 2012; Chery and Drouard, 2022). Moreover, tRNA sequences can act as transcriptional enhancers due to the promoter elements they contain, which can facilitate the recruitment of the RNA polymerase III (Dieci *et al.*, 2007; White, 2011). Taking advantage of this features, the tRNA-gRNA multiplexing system has been used successfully to increase gRNA transcript levels in rice protoplasts (Xie *et al.*, 2015) and to enhance the genome-editing efficiency in various other species such as maize, cotton, and sweet orange (Qi *et al.*, 2016; P. Wang *et al.*, 2018; Tang *et al.*, 2021).

The tRNA-gRNA system also reduces the complexity associated with constructing multiple independent gRNA expression cassettes. Previously, we have generated vectors as part of the OpenPlant kit (Sauret-Güeto *et al.*, 2020) that allow the introduction of both the Cas9 protein and up to two single-gRNA expression cassettes into the *M. polymorpha* genome via *Agrobacterium*-mediated plant transformation. In this study, we present an updated CRISPR/Cas9 vector system for *M. polymorpha* adapted from the OpenPlant kit that combines the Cas9 protein with a tRNA-gRNA module as a single transcript using a simple two-step cloning strategy. Furthermore, we combine the updated CRISPR/Cas9 vector system with an optimized and simplified protocol for *M. polymorpha* thallus transformation, eliminating the need for spores, which are often difficult and time-consuming to obtain. This approach further expands the ability to introduce multiple genetic modifications including large DNA deletions in the *M. polymorpha* wild type or mutant backgrounds.

In summary, we outline the generation and validation of constructs for gRNA multiplexing in *M. polymorpha*, providing a straightforward and efficient pipeline for multiplex gene editing and advanced plant engineering.

Material and methods

Plant material and growth conditions

Marchantia polymorpha accessions Cam-1 (male) and Cam-2 (female) (Delmans *et al.*, 2017) were used in this study. Plants were grown and maintained on half-strength Gamborg's B5 medium plus vitamins (DUCHEFA, #G0210.0050) and 1.2% (w/v) agar (Melford, Ipswich, UK; #A20021), under continuous light (80 µmol m^{-2} s^{-1}) at 21 °C.

Axenic cultures for spore production

Thallus fragments or gemmae were transferred into autoclaved microboxes containing 15 'Jiffy 7' pellets (Jiffy Products International B.V.), as previously described (Sauret-Güeto *et al.*, 2020). Briefly, 200 ml of water was added, and the plants were allowed to grow for 1 month under the conditions described above. Far-red light was then applied to induce the development of reproductive organs. Within 3–4 weeks, mature gametophores ready for fertilization became visible. For fertilization, a drop of sterile water was added to the male gametophore and the released sperm was transferred with a pipette onto the female gametophore. Mature sporophytes were visible and ready for collection after a month.

gRNA design

The design of the gRNAs was performed using the CasFinder tool (https://marchantia.info/tools/casfinder/). The program was run with the following configurations: CasFinder.pl -D -CONFIG CASFINDER_CONFIG.txt -CONFIG_CAS9 CASFINDER_CAS9_CONFIG_20.txt -g tak1_v5.1 -i query.fa -o out -A 1 -t 4. Searches were performed against the

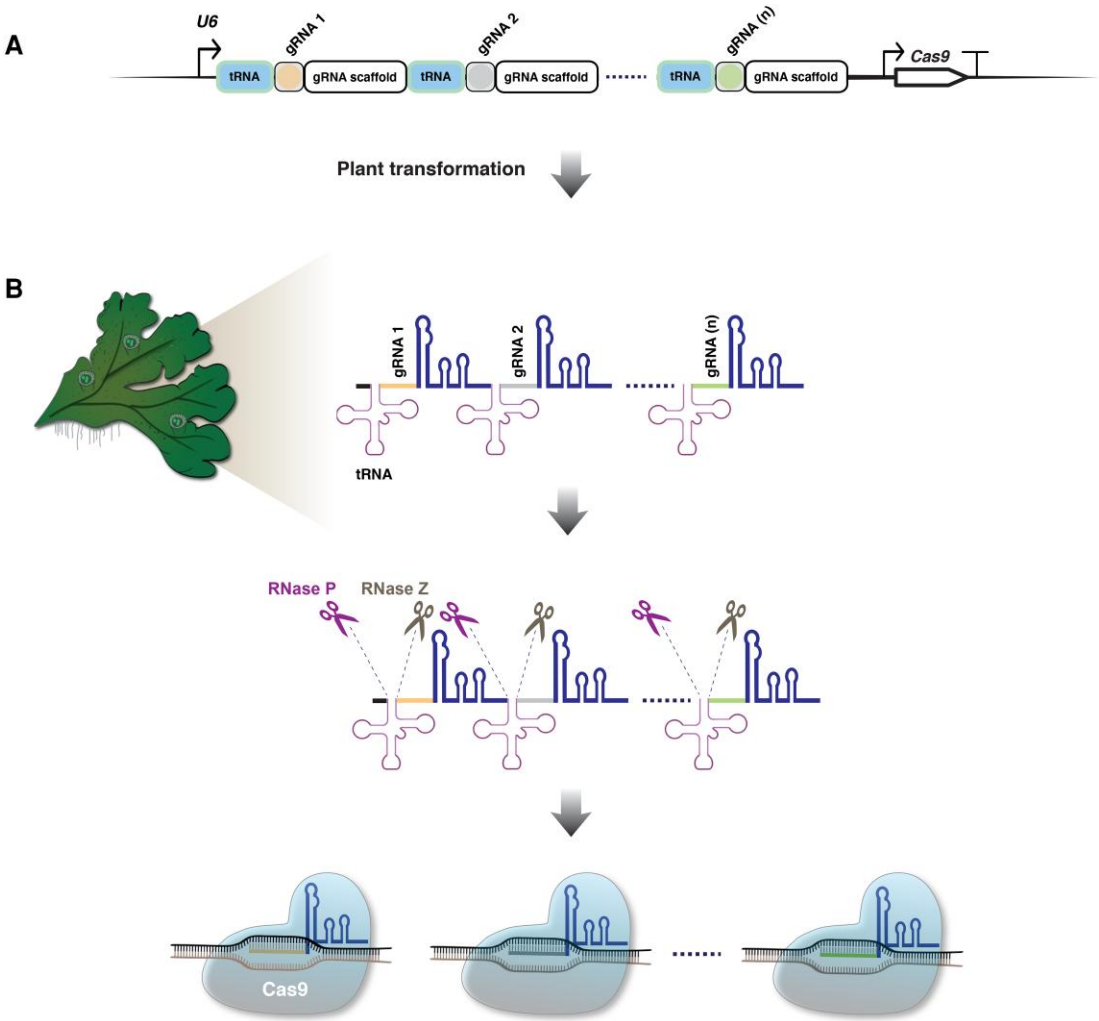

Fig. 1. Schematic diagram of tRNA-gRNA multiplexing for plant genome editing. (A) A plasmid is constructed containing a tRNA-gRNA cassette driven by the *U6* promoter, together with a transcription unit for Cas9 expression. (B) After transformation into the plant, the primary RNA transcript is cleaved by the endogenous tRNA-processing enzymes RNase P and RNase Z, resulting in functional guide RNAs for genome editing.

M. polymorpha Tak1 v5.1 genome, for 'Length of gRNA: 20 nt' and 'Primary/secondary PAM sequences: NGG/NAG'.

In vitro testing of gRNA

Primers were designed to amplify sequences containing the gRNA target DNA sequence (see Supplementary Table S1 and Supplementary Protocol S1). PCR was performed using Phusion DNA Polymerase (ThermoFisher Scientific; #F530S) and products from between two and five 50 µl reactions were pooled, and then purified using a QIAquick PCR Purification Kit (QIAGEN; #28104). Templates for *in vitro* transcription were generated by PCR using a forward primer containing the T7 promoter and crRNA sequence, a reverse primer matching the tracrRNA (Supplementary Table S1), and a plasmid template (pEn_Chimera, Addgene; plasmid #61432). Templates were purified with a QIAquick PCR Purification Kit.

cr-tracrRNA was synthesized using a MEGAscript™ T7 Transcription Kit (ThermoFisher Scientific; #AM1334). Transcription reactions were assembled following the manufacturer's protocol, with the following final volumes: 2 µl each of ATP, CTP, GTP, and UTP; 2 µl 10× Reaction Buffer; 2 µl Enzyme Mix; 0.1–1 µg of linear DNA template; and nuclease-free water to a final volume of 20 µl. Reactions were incubated at 37 °C for 16 h.

Following transcription, 0.5 µl of TURBO DNase (Invitrogen; #AM2238) was added to each reaction and incubated at 37 °C for 15 min to remove the DNA template. RNA was then purified using LiCl precipitation: 15 µl nuclease-free water and 15 µl LiCl Precipitation Solution (ThermoFisher Scientific; #AM1334) were added, mixed thoroughly, and

incubated at −20 °C for at least 30 min. RNA was pelleted by centrifugation at maximum speed (~10 000 *g*) for 15 min at 4 °C, washed once with 70% ethanol, and resuspended in 12 µl of nuclease-free water.

To test gRNA activity, *in vitro* cleavage assays were performed using recombinant Cas9 (NEB; #M0646T) and *in vitro*-transcribed gRNA. Reactions (30 µl total) contained 3 µl of 10× Cas9 Reaction Buffer, 3 µl of gRNA (~100 ng μl^{-1}), 0.15 µl of Cas9 (20 µM), and 3 µl of target DNA (200–300 ng), with nuclease-free water added to 30 µl. Prior to DNA addition, Cas9 and gRNA were pre-incubated for 10 min at 25 °C to allow complex formation. Reactions were incubated at 37 °C for 1 h, followed by addition of 1 µl Proteinase K and incubation at 65 °C for 10 min to degrade Cas9. Reactions were analysed immediately on agarose gels to assess cleavage efficiency.

Single-gRNA cloning into L1 vectors

Two oligo primers for cloning the gRNA target sequence were designed, as previously described (Sauret-Güeto *et al.*, 2020). To prepare the annealing reaction, 1 µl of each oligo (100 µM) was mixed with 8 µl of water to a final volume of 10 µl. The mixture was then annealed in a thermocycler under the following conditions: 37 °C for 30 min, 95 °C for 5 min, followed by a gradual decrease to 25 °C at a rate of 5 °C min^{-1}. After annealing, the gRNA target sequence was cloned into the L1_lacZgRNA-Ck2 and L1_lacZgRNA-Ck3 vectors (Addgene; #136137 and #136136, respectively). L1 BbsI-mediated Loop reactions were performed with minor modifications to the previous protocol of Sauret-Güeto *et al.* (2020). Briefly, the reaction included 1 µl of 7.5 nM of the L1_lacZgRNA-Ck2 or L1_lacZgRNA-Ck3 vector and 2 µl of annealed oligos. The Loop assembly Level 1 master mix contained 2 µl of 10× T4 DNA ligase buffer (NEB), 1.5 µl of 1 mg ml^{-1} BSA (NEB; #B9200S), 1.5 µl of T4 DNA ligase 400 U μl^{-1} (NEB; #M0202S), 1.5 µl of BbsI-HF 10 U μl^{-1} (NEB; #R3539), and nuclease-free H_2O to a final volume of 20 µl. The cycling conditions included 26 cycles of 37 °C for 3 min and 16 °C for 4 min, followed by enzyme inactivation at 50 °C for 5 min and 80 °C for 10 min. For transformation, 20 µl of chemically competent *E. coli* cells were incubated with 10 µl of the Loop assembly reaction and plated on LB agar containing 50 µg ml^{-1} kanamycin (Melford; #K22000–1.0) and 40 µg ml^{-1} X-Gal (ThermoFisher; #15520018).

Primer design for tRNA-gRNA module amplification

The tRNA-gRNA spacer-specific primers were designed with BbsI 4 bp overlapping overhangs for Golden Gate/Loop assembly. The sequences for these primers are as follows: G-primer-F (AGgaagacTACTCGAACAAAGCACCAGTGG) and 'gRNA c Primer R' (GAgaagacTATAAAAC-LAST-gRNA-REVcompl-TGCACCAGCCGGGAATC) (Fig. 2A). The sequences for 'gRNA a Primer F' and 'gRNA b Primer F' are GAgaagacAT-partial-gRNA-GTTTTAGAGCTAGAA, while 'gRNA a Primer R' and 'gRNA b Primer R' are GAgaagacTA-partial-gRNA-REVcompl-TGCACCAGCC-GGGAA. The primer combinations used for amplification (when three gRNAs are combined, but can be adapted to combine a larger number) are as follows: (1) G-primer-F with gRNA a Primer R, (2) gRNA a Primer F with gRNA b Primer R, and (3) gRNA b Primer F with gRNA c Primer R. The pGTR plasmid (Addgene; #63143) should be used as the template for these reactions. For detailed instructions and an example of primer design, see Supplementary Protocol S1 and https://dx.doi.org/10.17504/protocols.io.q26g7nx78lwz/v1. For PCR amplification, Phusion polymerase (ThermoFisher; #F534S) was used according to the manufacturer's instructions. The PCR products were gel-extracted using a QIAquick Gel Extraction Kit (QIAGEN, #28704).

tRNA-gRNA cloning into L1 vectors

To clone the tRNA-gRNA DNA fragments into either L1_lacZgRNA-Ck2 or L1_lacZgRNA-Ck3, the same procedure used for single-gRNA cloning was followed, with the only modification being the replacement of the annealed oligos with gel-extracted fragments. Reaction volumes were adjusted accordingly (see Supplementary Protocol S1 for detailed protocols).

L2 SapI-mediated Loop assembly

For the SapI-mediated Type IIS assembly, the following reaction was prepared: 2 µl of 10× T4 DNA ligase buffer (NEB), 1.5 µl of T4 DNA Ligase at 400 U μl^{-1} (NEB; #M0202S), 1.5 µl of SapI at 10 U μl^{-1} (NEB; #R0569S), 1 µl of 7.5 nM pCsA vector (Addgene; #136067), 1 µl of 15 nM L1 vectors, and nuclease-free H_2O to a final volume of 20 µl (see Supplementary Protocol S1 for detailed protocols). After assembly, 10 µl of the reaction mixture was transformed into *E. coli* and plated on LB agar containing 100 µg ml^{-1} spectinomycin (MERCK; #S4014-5G) and 40 µg ml^{-1} X-Gal for selection. The L1 vectors that used were: L1_Cas9-Ck4 containing the transcription unit for the Cas9 expression, (Addgene; #136135) (Sauret-Güeto *et al.*, 2020); L1_CsR-Ck1 (Plasmid #136124) or L1_HyR-Ck1 (Plasmid #136125; both Addgene) containing the transcription unit for chlorsulfuron or hygromycin selection, respectively; and if necessary the L1 spacer vectors pCk2_spacer or pCk3_spacer (Addgene; #136072 and #136073, respectively).

Agrobacterium culture preparation

LB medium (5 ml) supplemented with rifampicin 50 µg ml^{-1} (Duchefa; #R0146), gentamicin 25 µg ml^{-1} (Duchefa; #G0124), and spectinomycin 100 µg ml^{-1} (Bio Basic; #SB0901), were inoculated with 3–4 *Agrobacterium tumefaciens*

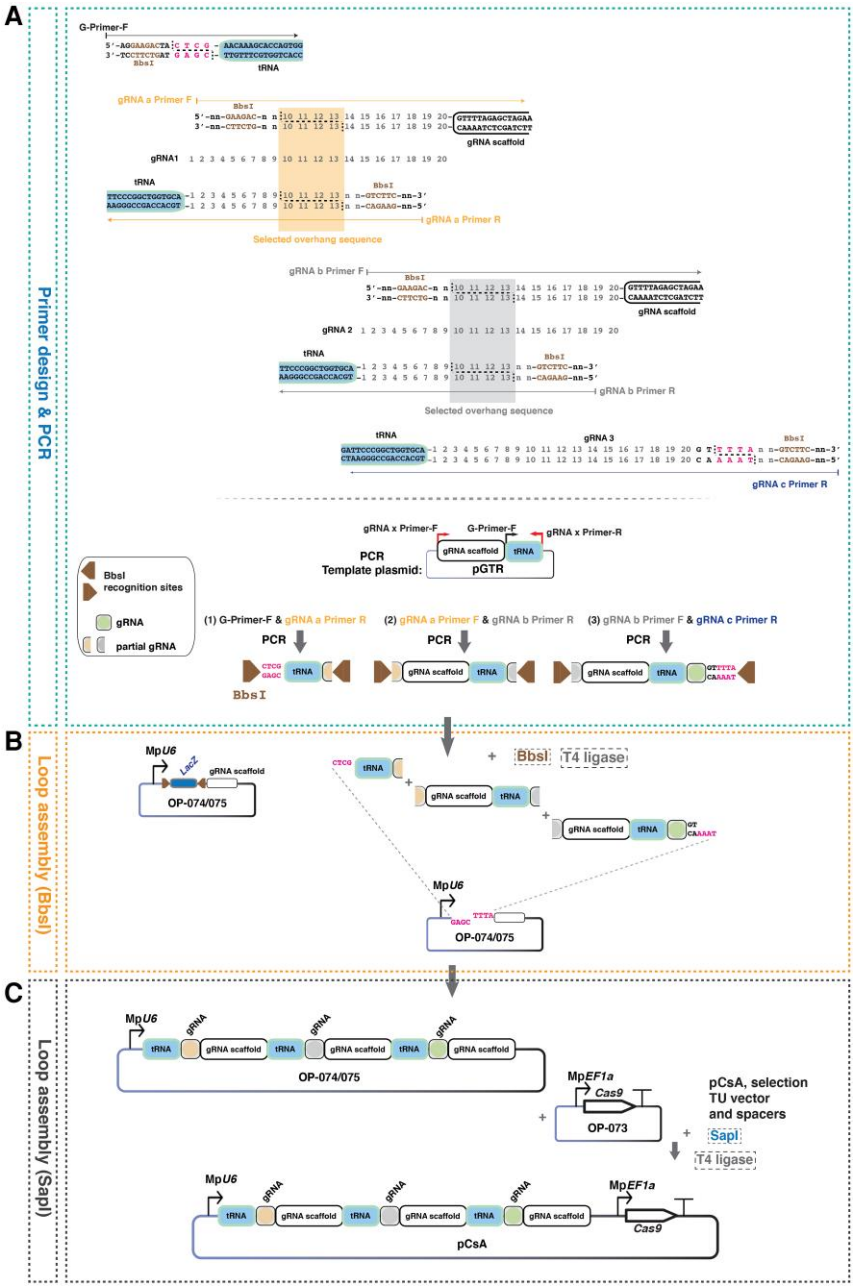

Fig. 2. Schematic diagram of the workflow for generating a tRNA-mediated multiplex gRNA expression construct. (A) Top: the first primer includes a portion of the tRNA sequence together with a BbsI recognition site and four-base overhang sequences for Loop assembly. The middle primers contain BbsI recognition sites and four-base overlapping overhang sequences for Loop assembly, which can correspond to any four consecutive nucleotides (highlighted by shading) within the 20-nucleotide gRNA sequence (numbered 1–20). The forward middle primers also contain a portion of the gRNA scaffold sequence, whereas the reverse middle primers contain a portion of the tRNA sequence. The final primer includes part of the tRNA sequence, the full reverse-complement of the last gRNA, and a BbsI recognition site plus four-base overhang sequences for Loop assembly. Overhangs for cloning into the acceptor vectors (CTCG and TTTA) shown with pink letters. n' represents any nucleotide. Bottom: the pGTR plasmid should be used as the template for the PCR reactions. The primer combinations used for amplification are as follows: (1) G-primer-F and gRNA a Primer R, (2) gRNA a Primer F and gRNA b Primer R, and (3) gRNA b Primer F and gRNA c Primer R. See Supplementary Protocol S1 for a detailed explanation and an example of primer design. (B) After PCR amplification and gel extraction, all fragments are combined with either the OP-074 or OP-075 vector (Sauret-Gueto *et al.*, 2020) in a Loop assembly/Type II S cloning reaction (see Supplementary Protocol S1 for a detailed description of Loop assembly L1 cloning). 'LacZ' represents the lacZα cassette for blue–white screening of colonies, where negative blue colonies contain undigested L1 vectors, whilst positive white colonies contain tRNA–gRNA parts inserted into the L1 vectors. (C) Finally, the tRNA–gRNA–OP-074 or –OP-075 vector is combined with the OP-073 vector (which contains the Mp*EF1a::Cas9* transcription unit) and with an appropriate L1 vector for plant selection in a Loop assembly/Type IIS cloning reaction (see Supplementary Protocol S1 for a detailed description of Loop Assembly L2 cloning).

colonies (GV3101). The preculture was incubated at 28 °C for 2 d with shaking at 100 rpm. After incubation (without measuring OD), 5 ml of the 2-day-old *Agrobacterium* culture was centrifuged at 2000*g* for 7 min. The supernatant was removed, and the pellet was resuspended in 5 ml of KNOP co-cultivation medium [0.25 g l^{-1} KH_2PO_4, 0.25 g l^{-1} KCl, 0.25 g l^{-1} $MgSO_4.7H_2O$, 1 g l^{-1} $Ca(NO_3)_2.4H_2O$, and 12.5 mg l^{-1} $FeSO_4.7H_2O$) containing 1% (w/v) sucrose (Melford; #S24060-1000.0) and 100 µM acetosyringone (4′-hydroxy-3′,5′-dimethoxyacetophenone) (MECK; #D134406). The culture was then incubated with shaking at 120 rpm at 28 °C for an additional 3–5 h.

Transformation procedure

Approximately 20 thallus cuttings, each around 2×2 mm–3×3 mm, were transferred into a 6-well plate containing 5 ml of liquid KNOP co-cultivation medium supplemented with 1% (w/v) sucrose, 30 mM MES (pH 5.5), 80 µl of *Agrobacterium* culture, and acetosyringone at a final concentration of 100 µM. The tissue was co-cultivated with *Agrobacterium* on a shaker at 110 rpm at 21–22 °C under ambient light (light intensity ~3–6 µmol m^{-2} $s^{-1)}$ for 3 d. After co-cultivation, the liquid was removed from the wells using a sterile plastic pipette, and the cuttings were transferred onto growth-medium plates containing the appropriate antibiotic, either hygromycin (Melford; #H7502) or chlorsulfuron (Sigma; #34322). To facilitate even distribution of thallus fragments on the plate, 2 ml of sterile water was added to each Petri dish. After 3–6 weeks, successful transformation events were observed as small, green regenerating tissue on dying or dead thallus fragments.

Genotyping

For genotyping, small pieces (3×3 mm) of thalli from individual plants were placed in 1.5 ml Eppendorf tubes and crushed with an autoclaved micropestle in 80 µl of genotyping buffer (100 mM Tris-HCl, 1 M KCl, and 10 mM EDTA, pH 9.5). The tubes were incubated at 70 °C for 25 min, followed by the addition of 350 µl of sterile water. A 2.5 µl aliquot of the extract was used as a template for PCR using Phusion polymerase (ThermoFisher; #F534S) or Quick Taq HS DyeMix (Toyobo; #DTM-101) following the manufacturer's instructions, and products were analysed on a 1.5% (w/v) agarose gel. The primers used for Mp*GLK* genotyping are listed in Supplementary Table S1. For Mp*rr-myb5* genotyping we used the primers described in Frangedakis *et al.* (2024).

Microscopy

For fluorescence microscopy a Leica M205 FA stereo microscope with fluorescence was used, equipped with the following filters: ET GFP (ET470/40 nm, ET525/50 nm) for observing eGFP, ET Chlorophyll LP (ET480/40 nm, ET610 nm LP) for chlorophyll, and ET GFP LP500 (ET470/40 nm, ET500 nm LP) for eGFP together with chlorophyll autofluorescence.

For light microscopy, images were captured using a Keyence VHX-S550E microscope (VHX-J20T lens).

Results

Synthesis of multiplex tRNA-gRNA modules using Type IIS cloning

We adapted the protocol originally developed for rice (Xie *et al.*, 2015) to clone tRNA-gRNA modules using the Loop assembly Type IIS cloning (Pollak *et al.*, 2019; Sauret-Güeto *et al.*, 2020) to enable efficient gene editing in *M. polymorpha* (Figs 1, 2). The process begins with primer design and PCR amplification of the tRNA-gRNA parts from the pGTR plasmid (Xie *et al.*, 2015; Addgene; #63143) that contains the tRNA and gRNA sequences (Fig. 2A). The PCR products contain the tRNA sequence, the gRNA scaffold, and a part of the gRNA protospacer sequence. These are then fused together to reconstitute multiplexed tRNA–gRNA-protospacer–gRNA-scaffold modules (up to three in our trials but the system allows the combination of a greater number) and placed under the control of the Mp*U6* promoter in an L1 vector (OpenPlant plasmids OP-074 or OP-075; Addgene #136136 or #136137, respectively; Sauret-Güeto *et al.*, 2020) via BbsI-mediated Loop assembly cloning (Fig. 2B). After transformation of the L1 Loop reaction into *E. coli* cells, screening 1–3 colonies was sufficient to identify correctly assembled constructs in our trials. Finally, the L1 tRNA-gRNA construct(s) is/are transferred into the L2 pCsA acceptor vector (Addgene #136067; Sauret-Güeto *et al.*, 2020) through another round of SapI-mediated Loop assembly (Fig. 2C), linking the tRNA-gRNA unit with the transcription unit for Cas9 expression (Addgene #136135; Sauret-Güeto *et al.*, 2020) and a transcription unit containing the desired selection marker. In summary, this protocol enables simple, fast, and efficient generation of constructs for targeted gene-editing in *M. polymorpha*, and reduces the number of experimental steps from seven to three compared with the original protocol (Xie *et al.*, 2015).

tRNA-gRNA multiplexing improves genome-editing efficiency by enabling the simultaneous delivery of multiple gRNAs

To test the efficiency of the new system, we targeted mutations in *M. polymorpha GOLDEN-2 LIKE* (Mp*GLK*), which lead to reduced levels of chlorophyll (Frangedakis *et al.*, 2024; Hernández-Muñoz *et al.*, 2024; Yelina *et al.*, 2024) and result in an easily observable, non-lethal phenotype that is useful for the evaluation of CRISPR/Cas9 efficiency. It also allows observation of the specific regions of the *M. polymorpha* thallus where mutations arise: knowing where mutations primarily arise is particularly important for identifying mutated areas of

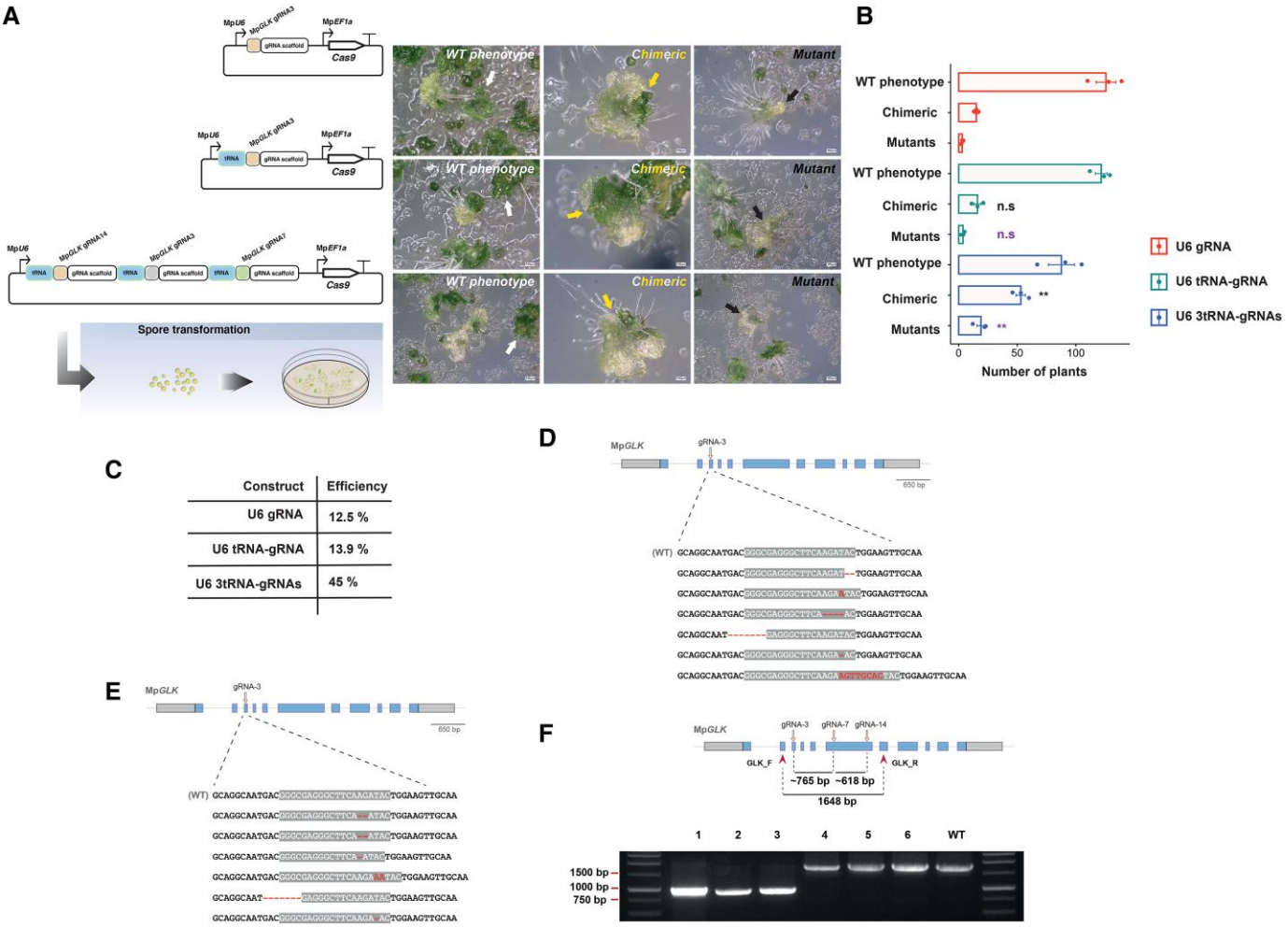

Fig. 3. Evaluation of mutant generation using the tRNA-mediated multiplex gRNA expression method. (A) Left: schematic representation of the plant transformation vectors for simultaneous delivery of either one or three gRNAs and Cas9 into *M. polymorpha* plants (germinating spores) by *Agrobacterium*-mediated transformation, with or without the use of tRNAs. Right: representative images of the three phenotypic classes of regenerating plants, indicated by arrows: wild-type (WT), chimeric, and mutant. Scale bars are 100 μm. (B) Comparison of the numbers of transformants with WT, chimeric, and mutant phenotypes generated using the control vector (U6 gRNA), the vector with one gRNA (U6 tRNA-gRNA), and the vector with three gRNAs (U6 3tRNA-gRNAs). Data are means (±SEM) of three independent experiments, with the individual data-points shown as dots. Significant differences compared with the control vector for the chimeric and mutant plants were determined using Student's *t*-test: $^{**}P<0.01$; n.s, not significant. (C) Quantification of the editing efficiency using the different vectors. (D, E) Sanger sequencing analysis of Mp*glk* mutant lines. Schematic representations of the Mp*GLK* gene structure showing exons as blue rectangles, untranslated regions (UTRs) as grey rectangles, and introns as grey lines. The position of the gRNA used for CRISPR/Cas9 gene editing is indicated. The sequence of the wild-type *M. polymorpha* Cam-1 accession is shown with the 20-bp gRNA target sequence highlighted in grey. Mutations are highlighted in red. (F) Gel electrophoresis of PCR-based genotyping of six Mp*glk* mutants obtained using the vector that allowed the expression of three gRNAs. The positions of primers used are indicated with arrowheads. The expected size of PCR products when large deletions occurred is ~600–800 bp (lanes 1–3). The expected size of PCR products for the WT and for mutants with small deletions is ~1648 bp (lanes 4–6, WT).

the plant when a gene mutation does not produce an obvious phenotype. In all our tests the *M. polymorpha* accession Cam-1/2 was used (Delmans *et al.*, 2017).

Using the tRNA-gRNA system, we constructed vectors to express either one (gRNA3) or three gRNAs (gRNA3, gRNA7, and gRNA14) to target the Mp*GLK* locus to generate large deletions (Fig. 3A). The selection of the three gRNAs was based on their *in vitro* activity in a cleavage assay that assessed their targeting performance (Supplementary Fig. S1A, B). Additionally, as a control we included a vector allowing gRNA3 expression from the commonly used Mp*U6* promoter without tRNA sequences (Fig. 3A). We transformed all three constructs into sporelings. In all cases, we observed regenerated thalli with pale green sectors, indicating successful disruption of Mp*GLK*. We classified the resulting plants into three distinct phenotypic categories: wild-type (WT), chimeric, and

fully mutant (Fig. 3A). For the control vector expressing gRNA3 without tRNA sequences, we observed ~88% WT, ~10% chimeric, and ~2% fully mutant plants (Fig. 3B), which was comparable to what was obtained when expressing the same gRNA3 with the tRNA sequences. Upon delivering the three gRNAs targeting Mp*GLK*, ~55% of the primary transformants exhibited the WT phenotype, ~33% were chimeric, and ~12% were fully mutant phenotypes. Overall, the editing efficiency was 12.5% when the gRNA was expressed without the presence of the tRNA sequences, 13.9% with the presence of tRNA sequences and a single gRNA, and 45% with multiple tRNA-gRNA modules (Fig. 3C). It must be noted that our approach to estimate the editing efficiency has the limitation that silent mutations are not calculated, and hence the actual editing efficiency is likely to be higher. To confirm successful gene disruption we performed Sanger sequencing, which validated the expected mutations (Fig. 3D, E; Supplementary Fig. S1C). We genotyped 60 independent mutant lines and found that 10% harbored large deletions (~600–800 bp, between gRNA3 and 7 or gRNA7 and 14; Fig. 3F; Supplementary Fig. S1C).

To further validate our new method, we also targeted the Mp*RR-MYB2* (Supplementary Fig. S2A), the mutation of which does not have a phenotype that differs from the WT plants (Supplementary Fig. S2B; Frangedakis *et al.*, 2024). We generated two vectors that allow the expression of a gRNA targeting the first exon with or without the presence of tRNA sequences (Supplementary Fig. S2C). We sequenced 34–40 independent lines transformed with each vector and ~11%–17.5% of the mutations did not alter the ORF (silent mutation; Supplementary Fig. S2C, D). The overall editing efficiency was between 73.5% and 82.5% when the gRNA was expressed without or with a tRNA sequence, respectively. This was higher compared to when we targeted Mp*GLK*, possibly due to the higher efficiency of the gRNA to target Cas9 to the desired loci.

Collectively, these results demonstrated a significant increase in gene-editing efficiency when using tRNA-gRNA multiplexing compared to vectors expressing a single gRNA, with or without tRNA. This enhanced efficiency is likely due to the ability of the system to deliver multiple gRNAs simultaneously and consequently to increase the chances of successfully targeting Cas9 to the desired loci.

A simplified and optimized thallus transformation method for *M. polymorpha*

Stable transformation of *M. polymorpha* can be obtained using either germinating spores or thallus fragments (Ishizaki *et al.*, 2008; Kubota *et al.*, 2013; Iwakawa *et al.*, 2021). Spore-based transformation offers high efficiency but requires ~3 months for spore production and can be challenging for certain accessions. Furthermore, transformants derived from spores consist of a mix of male and female plants and are not isogenic. In contrast, thallus transformation uses fragments or gemmalings as tissue material, which are more easily obtained than the spores and yield an isogenic population of transformants. Thallus transformation also allows the introduction of additional transgenes into specific mutant strains without segregation, as it bypasses sexual reproduction.

Here, we present a simplified protocol for *M. polymorpha* thallus transformation, adapted from a method originally developed for hornwort (Waller *et al.*, 2023). This protocol utilizes MES buffer to maintain a stable pH in the co-cultivation medium: maintaining a pH of 5.5 during co-cultivation has been shown to significantly enhance *Agrobacterium*-mediated infection in Arabidopsis and also hornworts, probably by inhibiting calcium-mediated defense signaling (Y-C. Wang *et al.*, 2018; Waller *et al.*, 2023). This optimized protocol omits the need for sucrose treatment of the regenerating tissue prior to co-cultivation with the *Agrobacterium* (Kubota *et al.*, 2013) and reduces the required volumes of co-cultivation media, effectively miniaturizing the process.

The protocol consists of the following steps (Fig. 4A, B; Supplementary Fig. S3A). Three 2-week-old gemmalings were transferred to one well of a 6-well plate containing 5 ml of liquid KNOP medium supplemented with 1% (w/v) sucrose and 10 mM MES, pH 5.5. The gemmalings were then cut into fragments with a scalpel (~20–25 fragments) and acetosyringone was added. The tissue was co-cultivated for 3 d on a shaker at 110 rpm under ambient light and 21 °C with *A. tumefaciens* carrying an *eGFP* gene fused to a cytoplasm-targeting signal and hygromycin-selectable marker gene (Fig. 4C). The thallus fragments were then transferred to growth media containing hygromycin or the selectable marker. Successful transformants, identifiable by eGFP fluorescence under a dissecting microscope, became visible from 3–6 weeks (Fig. 4C–G).

To further optimize the protocol, we evaluated the effect of MES concentration on transformation efficiency by adding it to the co-cultivation medium at concentrations ranging from 0–50 mM. eGFP fluorescence was used to estimate transformation efficiency. Increasing the MES concentration up to 30–40 mM resulted in more transformants, after which the number declined (Fig. 4H), and we considered the optimal concentration to be 30 mM. Interestingly, in many cases a single thallus fragment gave rise to more than one regenerated fragment/putative transformant (Fig. 4C); however not all regenerated fragments showed fluorescence, potentially due to partial T-DNA transfer or gene silencing (Fig. 4D–H). On average, we observed a transformation efficiency of ~30 transgenic plants per 20 fragments across different batches. All subsequent trials were performed using a MES concentration of 30 mM. The new method can be applied not only to gemmaling tissue but also to more mature thallus tissue, increasing the flexibility of our method and its ease of use. However, under our conditions, efficiency was reduced in older tissue (Supplementary Fig. S3B). To address this, scaling-up the protocol using

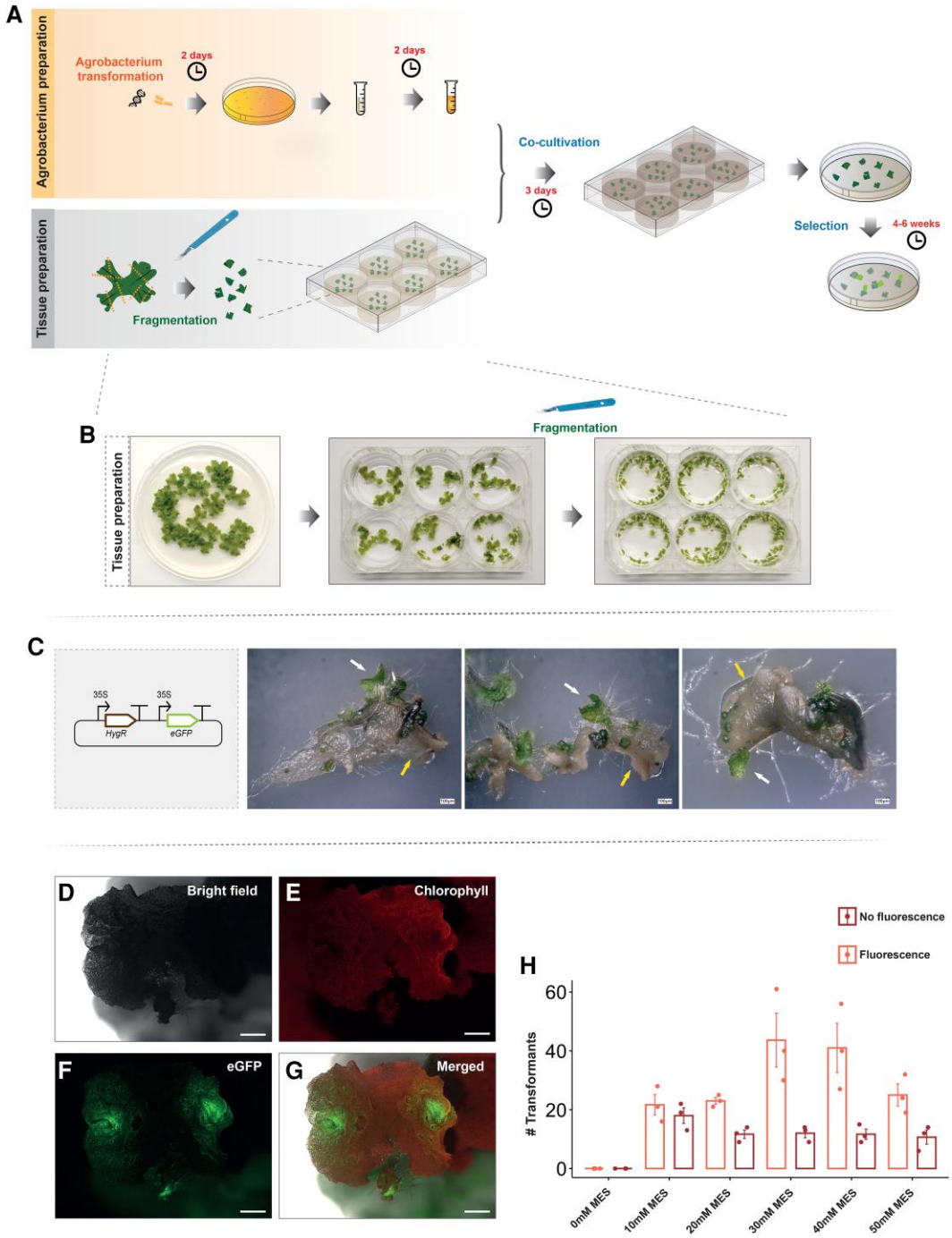

Fig. 4. An optimized protocol for *M. polymorpha* thallus transformation. (A) A schematic outline of the protocol steps. Thallus tissue is transferred into a 6-well plate containing 5 ml of co-cultivation medium and then cut inro fragments using a sterile scalpel. The tissue is co-cultivated with *Agrobacterium* for 3 d and then spread on growth medium containing antibiotics. After ~4–6 weeks, putative transformants are visible as regenerating green tissue. (B) Representative images of 2-week-old *M. polymorpha* gemmae, which are then transferred into the 6-well plate and fragmented prior to the addition of *Agrobacterium*. (C) Schematic representation of constructs for the expression of two transcription units, in this case one for the expression of the hygromycin gene (*HygR*) under the control of the cauliflower mosaic virus (CaMV) *35S* promoter, and one for the expression of *eGFP* also under the control of the CaMV *35S* promoter, and targeted to the plasma membrane using the Lti6b localization signal. Representative images are shown of thallus fragments after 4 weeks on antibiotic-containing growth medium, with regenerating tissue that is potentially successfully transformed indicated by white arrows. Untransformed, dying tissue is indicated with yellow arrows. Scale bars are 100 μm. (D–G) Images of thallus tissue expressing *35S::eGFP-Lti6b* for plasma membrane localization. Scale bars are 1 mm. (H) Comparison of the numbers of transformants per 20 thallus fragments under different MES concentrations in the co-cultivation medium (initial pH set to 5.5). Data are means (±SEM) of three independent experiments, with the individual data-points shown as dots.

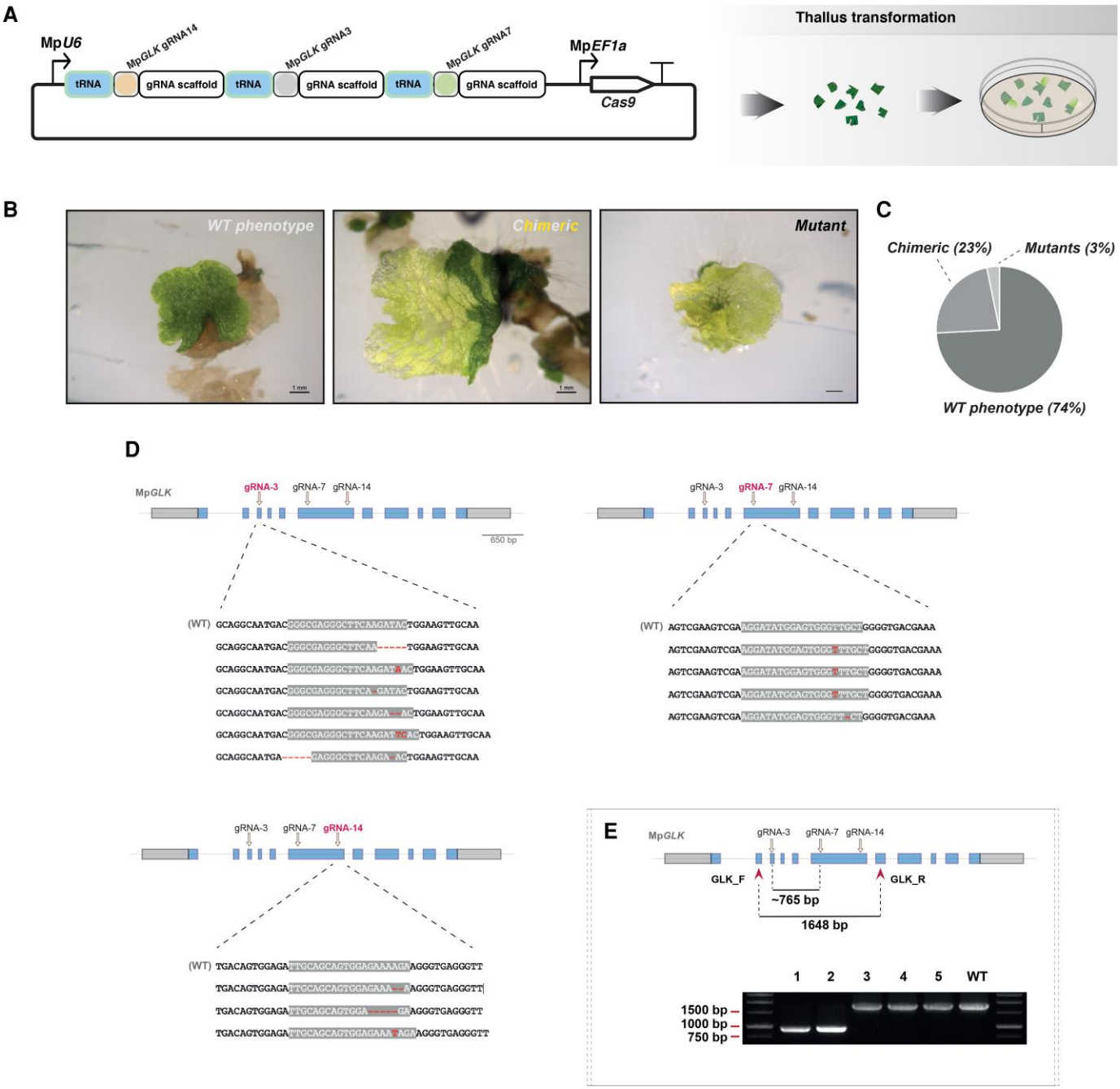

Fig. 5. Generation of *M. polymorpha* mutants using the optimized thallus transformation protocol. (A) Schematic representation of the plant transformation vector for simultaneous delivery of three gRNAs targeting Mp*GLK* and Cas9 into thallus fragments by *Agrobacterium*-mediated transformation, with or without the use of tRNAs. (B) Representative images of the three phenotypic classes of regenerated plants: wild-type (WT), chimeric, and mutant. Scale bars are 1 mm. (C) Proportions of transformants with WT, chimeric, or mutant phenotypes. *n*=100. (D) Sanger sequencing analysis of the Mp*glk* mutant lines. Schematic representations of the Mp*GLK* gene structure are shown, with exons indicated as blue rectangles, untranslated regions as grey rectangles, and introns as grey lines. The position of the gRNA used for CRISPR/Cas9 gene editing is shown with an arrow. The sequence of the wild-type *M. polymorpha* Cam-1 accession is shown with the 20-bp gRNA target sequence highlighted in grey. Mutations are highlighted in red. (E) Gel electrophoresis of PCR-based genotyping of five Mp*glk* mutants obtained using the vector that allows the expression of three gRNAs. A schematic representation of the Mp*GLK* gene structure is shown with the positions of the primers indicated. The expected size of PCR products when large deletions occur is ~765 bp (lanes 1 and 2). The expected size of PCR products for the WT and for mutants with small deletions is 1648 bp (lanes 3–5, WT).

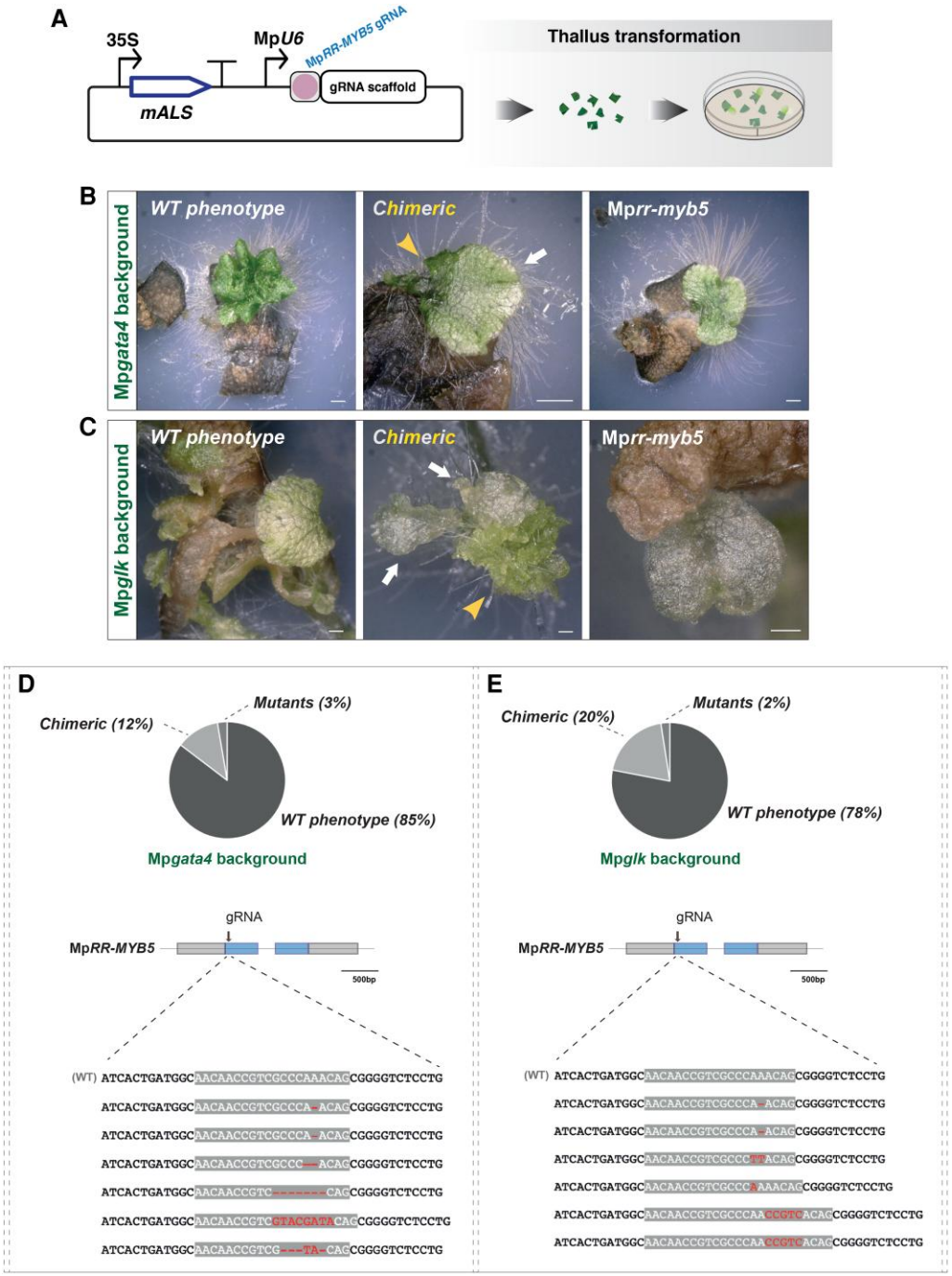

Fig. 6. Generation of *M. polymorpha* double-mutants using the optimized thallus transformation protocol. (A) Schematic representation of the plant transformation L2 vector for delivery of a gRNA targeting Mp*RR-MYB5* into thallus fragments of the desired mutant plant by *Agrobacterium*-mediated transformation. mALS, coding sequence for chlorsulfuron selection. (B, C) Representative images of the three phenotypic classes of regenerated plants observed in mutant plants transformed with the L2 vector targeting Mp*RR-MYB5*: wild type (WT), chimeric, and mutant. (B) Transformed plants in the Mp*gata4* mutant background and (C) in the Mp*glk* mutant background. Arrowheads indicate thallus parts with no visible mutation and arrows indicate thallus parts with a secondary mutation. Scale bars are 1 mm. (D, E) Proportions of transformants with WT, chimeric, or mutant phenotypes and Sanger sequencing analysis of the double-mutant lines. (D) Transformants in the Mp*gata4* mutant background and (E) in the Mp*glk* mutant background. The proportions of the phenotypes are based on *n*=100 transformants. The schematic representations of the Mp*RR-MYB5* gene structure show exons as blue rectangles, untranslated regions as grey rectangles, and introns as grey lines. The positions of gRNAs used for CRISPR/Cas9 gene editing are indicated. The sequences show the wild-type *M. polymorpha* Cam-1 accession at the top and the Mp*gata4 rr-myb5* and Mp*glk rr-myb5* double-mutants below, with the 20 bp gRNA target sequence highlighted with grey. Mutations are highlighted in red.

co-cultivation in flasks could be an alternative. Overall, our updated thallus transformation method facilitates the straightforward generation of isogenic transformants, offering a rapid approach for genetic studies and functional analyses in *M. polymorpha*.

The optimized thallus transformation procedure allows efficient generation of single- and double-mutants

Next, we tested whether our improved thallus transformation system could be used to obtain CRISPR/Cas9 mutants. To do this, we used the same vector as for the sporeling transformation trials to express the three gRNAs targeting Mp*GLK* (Fig. 5A). Similarly to sporeling transformation, the plants resulting from thallus transformation again fell into the three distinct phenotypic categories of WT, chimeric, and fully mutant (Fig. 5B). We transformed ∼200 thallus fragments and 74%, 23%, and 3% of the primary transformants exhibited WT, chimeric, and fully mutant phenotypes, respectively (Fig. 5C). Notably, the chimeric plants displayed multiple sectors with the mutant phenotype, indicating that mutations in each sector arose independently. The mutant sectors mostly appeared close to the meristematic notch (Supplementary Fig. S4A), possibly due to the stronger activity of the Mp*Ef1a* promoter that drives Cas9 expression in our constructs (Althoff *et al.*, 2014; Tse *et al.*, 2024). This observation is particularly valuable when a mutation does not result in an obvious phenotype, as tissues near the notch meristematic areas become top candidates for identifying mutant regions; however, we also found that mutant sectors could arise in more mature areas of the thallus (Supplementary Fig. S4B).

Successful gene disruption was confirmed by Sanger sequencing (Fig. 5D, E; Supplementary Fig. S1D). To evaluate the occurrence of large deletions, we genotyped 60 independent mutant lines and found that 2% carried a ∼765 bp deletion (gRNA3 and 7; Fig. 5E), which was confirmed by Sanger sequencing.

We also assessed whether our improved thallus transformation method could be used to generate double-mutants. In this approach, thalli from a mutant plant were subjected to secondary transformation using an L2 construct containing a different selectable marker and a transcription unit driving expression of a gRNA targeting a second gene, in this case Mp*RR-MYB5* (Fig. 6A). There was no need to include a separate transcription unit for Cas9 expression, as it was already present in the mutant background, simplifying the process. We selected Mp*RR-MYB5* as a target because, similar to Mp*GLK*, its mutation leads to reduced chlorophyll and therefore it is an easily observable, non-lethal phenotype ideal for the evaluation of gene-editing efficiency (Frangedakis *et al.*, 2024). We targeted Mp*RR-MYB5* in two different mutant backgrounds, M*pgata4* and Mp*glk* (Yelina *et al.*, 2024), that have distinct thallus morphologies and phenotypes in order to test the effectiveness of our protocol across varying mutant types. The resulting plants again fell into the three distinct phenotypic categories of the original background genotype, chimeric, and fully mutant (Fig. 6B, C). Of the recovered transformants in the Mp*gata4* background (n=100), 85% were wild type for Mp*RR-MYB5*, 12% were chimeric, and 3% were fully mutant for Mp*rr-myb5* (Fig. 6D). Out of the transformants recovered from transforming the Mp*glk* mutant thallus fragments (n=100), 78% were wild type for Mp*RR-MYB5*, 20% were chimeric, and 2% were fully mutant for Mp*rr-myb5* (Fig. 6E). Successful gene disruption was confirmed by Sanger sequencing.

We also investigated whether our system could achieve simultaneous disruption of two genes using thallus tissue as the transformation material. To this end, we selected Mp*GLK* and Mp*RR-MYB5* and constructed a plasmid allowing the expression of two gRNAs, each specifically targeting one of the genes (Supplementary Fig. S5A). Following transformation, we obtained single-mutants for Mp*glk* (20%) and Mp*rr-myb5* (9.8%), as well as double-mutants harboring disruptions in both genes, Mp*glk rr-myb5* (3.2%) (Supplementary Fig. S5B, C). After allowing the plants to grow for an additional 2 weeks, we observed the emergence of several secondary mutations, predominantly localized in the meristematic regions (Supplementary Fig. S5B–D). Approximately 17.5% of the meristematic areas contained secondary double-mutations (Supplementary Fig. S5E).

Collectively, our results demonstrate that the optimized thallus transformation system is a reliable and efficient method for generating both single and double CRISPR/Cas9-mediated mutants, including in mutant backgrounds with altered thallus tissue morphology or development.

Conclusions

CRISPR-based genome editing tools have significantly advanced biology (Chen *et al.*, 2019; Wang and Doudna, 2023; Pacesa *et al.*, 2024), and their application to *M. polymorpha* has substantially enhanced its utility as a model organism (Sugano *et al.*, 2014, 2018; Sauret-Güeto *et al.*, 2020). In this study, we successfully adapted gRNA multiplexing by expressing gRNAs from a single transcriptional tRNA-gRNA unit (Xie *et al.*, 2015) for CRISPR/Cas9 genome editing in *M. polymorpha*. By incorporating tRNA sequences into the OpenPlant CRISPR/Cas9 kit vector system, we have demonstrated that the tRNA-gRNA approach results in functional gRNAs. Importantly, our approach for cloning the tRNA-gRNA module into the transformation vector is significantly simplified and can also be adapted to other *M. polymorpha* CRISPR/Cas9 vector systems.

Our approach streamlines genome editing in *M. polymorpha*, allowing the introduction of multiple modifications and deletion of large DNA fragments in single or multiple loci, in a single transformation event. Furthermore, when combined with our optimized thallus transformation protocol, our new method simplifies mutant generation by eliminating the need for spore production, which takes ∼2–3 months. This is

particularly useful for generating secondary mutations in mutant backgrounds, especially for those that are unable to produce spores. Targeting genes for which the mutation generates a visible phenotype allowed us to identify the notch regions in the *M. polymorpha* thallus as areas where mutations occur more often. This observation can facilitate the identification of edited parts of the plant when a mutation does not result in an obvious phenotype.

Beyond fundamental research, *M. polymorpha* is a promising chassis for synthetic biology applications (Boehm *et al.*, 2017; Sauret-Güeto *et al.*, 2020; Frangedakis *et al.*, 2021). It offers several advantages, including a relatively fast life cycle, simpler tissue organization compared with other plant models, and well-characterized nuclear and plastid genomes that are both amenable to genetic manipulation and high-throughput approaches (Annese *et al.*, 2025). To date, five different selectable markers have been tested in *M. polymorpha*, further expanding the capacity to introduce multiple transgenes (Ishizaki *et al.*, 2015; Robinson *et al.*, 2024). All these can facilitate the reprogramming of gene regulatory networks with high precision and speed. Moreover, *M. polymorpha* can potentially serve as a platform for testing and developing novel biotechnological tools, such as biosensors, bio-based production of high-value compounds, and cell-type-specific metabolic engineering (Yang and Reyna-Llorens, 2023; Tansley *et al.*, 2024). Its ability to produce complex secondary metabolites further enhances its potential for bioengineering (Forestier *et al.*, 2025, Preprint; Lindström Battle and Sweetlove, 2025). As a result, developing improved CRISPR/Cas9 tools in *M. polymorpha* can significantly enhance the versatility of genome-engineering approaches in this model system. One promising strategy involves the use of tRNA-based expression systems for gRNAs, which enables their transcription under *RNA polymerase II* (*Pol II*) promoters. Unlike traditional *U6* promoters, which are transcribed by RNA polymerase III and drive constitutive, ubiquitous expression, *Pol II* promoters offer greater regulatory flexibility. This includes the ability to achieve cell-type-specific or inducible expression of gRNAs, thereby allowing spatial and temporal control over genome-editing activity, building on recent work on the landscape of transcription-factor promoter activity in *M. polymorpha* (Romani *et al.*, 2024). It can also allow the exploration of CRISPR-based multiplex gene regulation systems to simultaneously control the expression of multiple genes in a coordinated way. One notable application of multiplexing is metabolic pathway optimization, where several enzymes within a biosynthetic pathway are concurrently modulated to enhance the production of valuable compounds.

In conclusion, our study establishes an improved genome-editing approach for *M. polymorpha* by using the tRNA-gRNA multiplexing system. This strategy enables the simultaneous delivery of multiple gRNAs into the plant, facilitating the editing of single genes or multiple loci in parallel. Our method not only enhances editing efficiency but also expands the potential for more complex genetic modifications in *M. polymorpha*, laying the groundwork for advanced functional genomics and synthetic biology applications in this model organism.

Supplementary data

The following supplementary data are available at *JXB* online.

Fig. S1. *In vitro* test of Mp*GLK* gRNAs and genotyping results.
Fig. S2. Generation of Mp*RR-MYB2* mutants.
Fig. S3. Key steps of the optimized thallus transformation procedure.
Fig. S4. Images of chimeric Mp*glk* mutants.
Fig. S5. Generation of Mp*glk rr-myb5* double-mutants.
Table S1. List of primers used in this study.
Protocol S1. Generation of multiplex tRNA-gRNA constructs for CRISPR/Cas9 editing of *M. polymorpha*.

Acknowledgements

We thank Keiko Sakakibara from Rikkyo University, Japan, for her support during the later stages of the project.

Author contributions

EF and NYE. designed the study; EF, NYE, SKE, FR, and AF, carried out the experimental work; JH and JMH oversaw the project; EF wrote the manuscript with input from all the authors.

Conflict of interest

The authors declare that they have no conflicts of interest in relation to this work.

Funding

This work was funded by BBSRC grant no. BB/L014130/1 to JH as part of the OpenPlant Synthetic Biology Research Centre BBSRC grant no. BB/F011458/1 for confocal microscopy to JH, and grant no. BBP0031171 to JMH.

Data availability

All data supporting the conclusions of this study are contained within the manuscript and its supplementary materials published online. A detailed protocol can also be found at https://dx.doi.org/10.17504/protocols.io.q26g7nx78lwz/v1 (Frangedakis, 2025a). A plasmid map is openly available in Zenodo at https://doi.org/10.5281/zenodo.17191738 (Frangedakis, 2025b).

References

Adli M. 2018. The CRISPR tool kit for genome editing and beyond. Nature Communications **9**, 1911.

Althoff F, Kopischke S, Zobell O, Ide K, Ishizaki K, Kohchi T, Zachgo S. 2014. Comparison of the *MpEF1α* and *CaMV35* promoters for application in *Marchantia polymorpha* overexpression studies. Transgenic Research **23**, 235–244.

Annese D, Romani F, Grandellis C, Ives L, Frangedakis E, Buson FX, Molloy JC, Haseloff J. 2025. Semi-automated workflow for high-throughput *Agrobacterium*-mediated plant transformation. The Plant Journal **122**, e70118.

Boehm CR, Pollak B, Purswani N, Patron N, Haseloff J. 2017. Synthetic botany. Cold Spring Harbor Perspectives in Biology **9**, a023887.

Bowman JL, Arteaga-Vazquez M, Berger F, *et al.* 2022. The renaissance and enlightenment of *Marchantia* as a model system. The Plant Cell **34**, 3512–3542.

Čermák T, Curtin SJ, Gil-Humanes J, *et al.* 2017. A multipurpose toolkit to enable advanced genome engineering in plants. The Plant Cell **29**, 1196–1217.

Chen K, Wang Y, Zhang R, Zhang H, Gao C. 2019. CRISPR/Cas genome editing and precision plant breeding in agriculture. Annual Review of Plant Biology **70**, 667–697.

Chery M, Drouard L. 2022. Plant tRNA functions beyond their major role in translation. Journal of Experimental Botany **74**, 2352–2363.

Cong L, Ran FA, Cox D, *et al.* 2013. Multiplex genome engineering using CRISPR/Cas systems. Science **339**, 819–823.

Delmans M, Pollak B, Haseloff J. 2017. MarpoDB: an open registry for *Marchantia polymorpha* genetic parts. Plant & Cell Physiology **58**, e5.

Dieci G, Fiorino G, Castelnuovo M, Teichmann M, Pagano A. 2007. The expanding RNA polymerase III transcriptome. Trends in Genetics **23**, 614–622.

Donà M, Bradamante G, Bogojevic Z, Gutzat R, Streubel S, Mosiolek M, Dolan L, Mittelsten Scheid O. 2023. A versatile CRISPR-based system for lineage tracing in living plants. The Plant Journal **115**, 1169–1184.

Forestier ECF, Asprilla P, Romani F, Bonter I, Frangedakis E, Haseloff J. 2025. The ABCG1 transporter facilitates sesquiterpene accumulation in *Marchantia polymorpha* oil bodies. bioRxiv doi: 10.1101/2025.02.05.636625. [Preprint].

Frangedakis E, Guzman-Chavez F, Rebmann M, *et al.* 2021. Construction of DNA tools for hyperexpression in *Marchantia* chloroplasts. ACS Synthetic Biology **10**, 1651–1666.

Frangedakis E, Yelina NE, Billakurthi K, Hua L, Schreier T, Dickinson PJ, Tomaselli M, Haseloff J, Hibberd JM. 2024. MYB-related transcription factors control chloroplast biogenesis. Cell **187**, 4859–4876.e22.

Frangedakis E. 2025a. Generation of multiplex tRNA-gRNA constructs for *Marchantia polymorpha* CRISPR. protocols.io. https://dx.doi.org/10.17504/protocols.io.q26g7nx78lwz/v1

Frangedakis E. 2025b. l2-glk-3g-csa.gb plasmid. Zenodo. https://doi.org/10.5281/zenodo.17191739

Gupta OP, Karkute SG. 2021. Genome editing in plants: principles and applications. Boca Raton, FL: CRC Press.

Hernández-Muñoz A, Agreda-Laguna KA, Ramírez-Bernabé IE, Oltehua-López O, Arteaga-Vázquez MA, Leon P. 2024. *Marchantia polymorpha* GOLDEN2-LIKE transcriptional factor; a central regulator of chloroplast and plant vegetative development. New Phytologist **243**, 1406–1423.

Hui L, Zhao M, He J, *et al.* 2019. A simple and reliable method for creating PCR-detectable mutants in Arabidopsis with the polycistronic tRNA–gRNA CRISPR/Cas9 system. Acta Physiologiae Plantarum **41**, 170.

Ishizaki K, Chiyoda S, Yamato KT, Kohchi T. 2008. *Agrobacterium*-mediated transformation of the haploid liverwort *Marchantia polymorpha* L., an emerging model for plant biology. Plant & Cell Physiology **49**, 1084–1091.

Ishizaki K, Nishihama R, Ueda M, Inoue K, Ishida S, Nishimura Y, Shikanai T, Kohchi T. 2015. Development of gateway binary vector series with four different selection markers for the liverwort *Marchantia polymorpha*. PLoS ONE **10**, e0138876.

Ishizaki K, Nishihama R, Yamato KT, Kohchi T. 2016. Molecular genetic tools and techniques for *Marchantia polymorpha* research. Plant & Cell Physiology **57**, 262270.

Iwakawa H, Melkonian K, Schlüter T, Jeon H-W, Nishihama R, Motose H, Nakagami H. 2021. *Agrobacterium*-mediated transient transformation of *Marchantia* liverworts. Plant & Cell Physiology **62**, 1718–1727.

Jinek M, Chylinski K, Fonfara I, Hauer M, Doudna JA, Charpentier E. 2012. A programmable dual-RNA-guided DNA endonuclease in adaptive bacterial immunity. Science **337**, 816–821.

Kocaoglan EG, Radhakrishnan D, Nakayama N. 2023. Synthetic developmental biology: molecular tools to re-design plant shoots and roots. Journal of Experimental Botany **74**, 3864–3876.

Kohchi T, Yamato KT, Ishizaki K, Yamaoka S, Nishihama R. 2021. Development and molecular genetics of *Marchantia polymorpha*. Annual Review of Plant Biology **72**, 677–702.

Kubota A, Ishizaki K, Hosaka M, Kohchi T. 2013. Efficient *Agrobacterium*-mediated transformation of the liverwort *Marchantia polymorpha* using regenerating thalli. Bioscience, Biotechnology, and Biochemistry **77**, 167–172.

Lindström Battle AL, Sweetlove LJ. 2025. Bryophytes as metabolic engineering platforms. Current Opinion in Plant Biology **85**, 102702.

Ma C, Zhu C, Zheng M, Liu M, Zhang D, Liu B, Li Q, Si J, Ren X, Song H. 2019. CRISPR/Cas9-mediated multiple gene editing in *Brassica oleracea* var. *capitata* using the endogenous tRNA-processing system. Horticulture Research **6**, 20.

Naramoto S, Hata Y, Fujita T, Kyozuka J. 2022. The bryophytes *Physcomitrium patens* and *Marchantia polymorpha* as model systems for studying evolutionary cell and developmental biology in plants. The Plant Cell **34**, 228–246.

Pacesa M, Pelea O, Jinek M. 2024. Past, present, and future of CRISPR genome editing technologies. Cell **187**, 1076–1100.

Pollak B, Cerda A, Delmans M, Álamos S, Moyano T, West A, Gutiérrez RA, Patron NJ, Federici F, Haseloff J. 2019. Loop assembly: a simple and open system for recursive fabrication of DNA circuits. New Phytologist **222**, 628–640.

Qi W, Zhu T, Tian Z, Li C, Zhang W, Song R. 2016. High-efficiency CRISPR/Cas9 multiplex gene editing using the glycine tRNA-processing system-based strategy in maize. BMC Biotechnology **16**, 58.

Ran FA, Hsu PD, Wright J, Agarwala V, Scott DA, Zhang F. 2013. Genome engineering using the CRISPR-Cas9 system. Nature Protocols **8**, 2281–2308.

Robinson K, Chia K-S, Guyon A, Schornack S, Carella P. 2024. An efficient sulfadiazine selection scheme for stable transformation in the model liverwort *Marchantia polymorpha*. Journal of Experimental Botany **75**, 5585–5591.

Romani F, Sauret-Güeto S, Rebmann M, *et al.* 2024. The landscape of transcription factor promoter activity during vegetative development in *Marchantia*. The Plant Cell **36**, 2140–2159.

Sauret-Güeto S, Frangedakis E, Silvestri L, Rebmann M, Tomaselli M, Markel K, Delmans M, West A, Patron NJ, Haseloff J. 2020. Systematic tools for reprogramming plant gene expression in a simple model, *Marchantia polymorpha*. ACS Synthetic Biology **9**, 864–882.

Sugano SS, Shirakawa M, Takagi J, Matsuda Y, Shimada T, Hara-Nishimura I, Kohchi T. 2014. CRISPR/Cas9-mediated targeted mutagenesis in the liverwort *Marchantia polymorpha* L. Plant & Cell Physiology **55**, 475–481.

Sugano SS, Nishihama R, Shirakawa M, Takagi J, Matsuda Y, Ishida S, Shimada T, Hara-Nishimura I, Osakabe K, Kohchi T. 2018. Efficient CRISPR/Cas9-based genome editing and its application to conditional genetic analysis in *Marchantia polymorpha*. PLoS ONE **13**, e0205117.

Tang X, Chen S, Yu H, Zheng X, Zhang F, Deng X, Xu Q. 2021. Development of a gRNA–tRNA array of CRISPR/Cas9 in combination with grafting technique to improve gene-editing efficiency of sweet orange. Plant Cell Reports **40**, 2453–2456.

Tansley C, Patron NJ, Guiziou S. 2024. Engineering plant cell fates and functions for agriculture and industry. ACS Synthetic Biology **13**, 998–1005.

Tse SW, Annese D, Romani F, Guzman-Chavez F, Bonter I, Forestier E, Frangedakis E, Haseloff J. 2024. Optimizing promoters and subcellular localization for constitutive transgene expression in *Marchantia polymorpha*. Plant & Cell Physiology **65**, 1298–1309.

Waller M, Frangedakis E, Marron AO, Sauret-Güeto S, Rever J, Sabbagh CRR, Hibberd JM, Haseloff J, Renzaglia KS, Szövényi P. 2023. An optimized transformation protocol for *Anthoceros agrestis* and three more hornwort species. The Plant Journal **114**, 699–718.

Wang JY, Doudna JA. 2023. CRISPR technology: a decade of genome editing is only the beginning. Science **379**, eadd8643.

Wang P, Zhang J, Sun L, *et al.* 2018. High efficient multisites genome editing in allotetraploid cotton (Gossypium hirsutum) using CRISPR/Cas9 system. Plant Biotechnology Journal **16**, 137–150.

Wang Y-C, Yu M, Shih P-Y, Wu H-Y, Lai E-M. 2018. Stable pH suppresses defense signaling and is the key to enhance *Agrobacterium*-mediated transient expression in Arabidopsis seedlings. Scientific Reports **8**, 17071.

Wang Z, Liu X, Xie X, Deng L, Zheng H, Pan H, Li D, Li L, Zhong C. 2021. ABE8e with polycistronic tRNA–gRNA expression cassette significantly improves adenine base editing efficiency in *Nicotiana benthamiana*. International Journal of Molecular Sciences **22**, 5663.

White RJ. 2011. Transcription by RNA polymerase III: more complex than we thought. Nature Reviews Genetics **12**, 459–463.

Wilusz JE, JnBaptiste CK, Lu LY, Kuhn C-D, Joshua-Tor L, Sharp PA. 2012. A triple helix stabilizes the 3′ ends of long noncoding RNAs that lack poly(A) tails. Genes & Development **26**, 2392–2407.

Xie K, Minkenberg B, Yang Y. 2015. Boosting CRISPR/Cas9 multiplex editing capability with the endogenous tRNA-processing system. Proceedings of the National Academy of Sciences, USA **112**, 3570–3575.

Yang J-S, Reyna-Llorens I. 2023. Plant synthetic biology: exploring the frontiers of sustainable agriculture and fundamental plant biology. Journal of Experimental Botany **74**, 3787–3790.

Yelina NE, Frangedakis E, Wang Z, *et al.* 2024. Streamlined regulation of chloroplast development in the liverwort *Marchantia polymorpha*. Cell Reports **43**, 114696.